International Journal of Nanomedicine

Dovepress
open access to scientific and medical research

Open Access Full Text Article

ORIGINAL RESEARCH

Vesicular melatonin efficiently downregulates sodium fluoride-induced rat hepato- and broncho-TNF-α, TGF-β expressions, and associated oxidative injury: a comparative study of liposomal and nanoencapsulated forms

This article was published in the following Dove Press journal:
International Journal of Nanomedicine
29 May 2017
Number of times this article has been viewed

Suvomoy Sana
Swarupa Ghosh
Nirmalendu Das
Sibani Sarkar
Ardhendu Kumar Mandal

Drug Development, Diagnostics and Biotechnology, CSIR-Indian Institute of Chemical Biology, West Bengal, India

Abstract: The importance of fluoride as a natural and industrial toxicant is recognized worldwide. We evaluated the regulating role and biological effect of vesicular (liposomal and nanoencapsulated) melatonin (N-acetyl-5-methoxytryptamine) for drug delivery and controlled release on the depletion of inflammatory mediators, as well as oxidative damage in sodium fluoride (NaF)-treated lungs and liver. Hepatic and bronchial damage was induced in Swiss albino rats with a single acute ingestion of NaF (48 mg/kg body weight, oral gavage). NaF exposure caused the generation of reactive oxygen species (ROS); upregulation of TNF-α and TGF-β; decreased activities of antioxidant systems (glutathione, glutathione-S-transferase, superoxide dismutase, catalase), succinate dehydrogenase, membrane microviscosity, and membrane potential; increased activity of lipid peroxidation and nicotinamide adenine dinucleotide hydride oxidase; and increased hepatic and nephrite toxicities ($P<0.001$) compared to those in normal animals. Charge (−ve/+ve)-specific single liposomal (dicetyl phosphate/stearylamine) and nanoencapsulated melatonin (4.46 mg/kg body weight, intravenous) treatments (2 hours after NaF exposure) significantly ($P<0.01/0.001$) and maximally ($P<0.001$) inhibited all alterations developed in NaF-mediated oxidative injuries in rat liver (+ve) and lungs (−ve), demonstrating their strong free radical scavenging, antioxidant and antigenotoxic properties, and vesicular efficiencies of targeting. Overall, these results suggest that nanoencapsulated melatonin might be considered as a more powerful remedial therapy in comparison to liposomes, in terms of its efficacy in regulating NaF-intoxicated oxidative injury.

Keywords: sodium fluoride, reactive oxygen species, inflammatory mediators, oxidative injury, vesicular melatonin targeting

Introduction

Fluorine, being the most electronegative element, reacts with other elements to form ionized fluorides.[1] Fluorides are found widely in food of both animal and plant origin due to their extensive prevalence in air, soil, and water and are an important environmental pollutant arising from natural and industrial sources.[2] Living organisms come in contact with fluoride through food, drinking water, fluoride additives, toothpastes, fluoride gel,[3] and inhalation of hydrofluoric gases through smoke, vapors, dust from burning coal, industrial manufacture of phosphate fertilizers, and volcanoes.[4] Fluoride, on entering soft tissues after crossing cell membranes by simple diffusion,

Correspondence: Ardhendu Kumar Mandal
CSIR-Indian Institute of Chemical Biology, 4, Raja SC Mullick Road, Jadavpur, Kolkata 700032, West Bengal, India
Tel +91 33 2499 5879
Fax +91 33 2473 5197
Email ardhendu_mandal@yahoo.co.in

submit your manuscript | www.dovepress.com
Dovepress
http://dx.doi.org/10.2147/IJN.S124119

© 2017 Sana et al. This work is published and licensed by Dove Medical Press Limited. The full terms of this license are available at https://www.dovepress.com/terms.php and incorporate the Creative Commons Attribution – Non Commercial (unported, v3.0) License (http://creativecommons.org/licenses/by-nc/3.0/). By accessing the work you hereby accept the Terms. Non-commercial uses of the work are permitted without any further permission from Dove Medical Press Limited, provided the work is properly attributed. For permission for commercial use of this work, please see paragraphs 4.2 and 5 of our Terms (https://www.dovepress.com/terms.php).

causes impairment.[5] Drinking water contains ionic fluoride that crosses the intestinal mucosa by passive diffusion, and initiates oxidative stress and inflammation and causes development of fluorosis, causing damage of the soft tissues.

Fluoride in aqueous solution ingested orally is converted to hydrogen fluoride (HF) in the acidic conditions of the stomach, and is transported to blood from the stomach as HF.[6] Fluoride is then distributed throughout the body by a mechanism of pH gradient-dependent transport, where the neutral HF penetrates the cell membrane through non-ionic diffusion. High amounts of sodium fluoride (NaF) are known to cause configurational alterations and altered enzyme activity in cells, and to influence lipid metabolism.[7] Acute NaF poisoning may result in death because of blocked cell metabolism.[8] Recent studies have revealed the NaF-induced production of ROS and subsequent reduced functions of some antioxidant enzymes.[9] It is postulated that increased ROS, lipid peroxidation, altered antioxidant defense system, and inflammation may attribute to the poisonous effects of NaF in soft tissues such as liver and lungs.[10] Fluoride can activate microglia, the resident macrophages, and release ROS and pro-inflammatory factors, for example, TGF-β and TNF-α, characterized as modulators for various mammalian intracellular signaling pathways.[11]

Measures to prevent and treat fluoride-induced oxidative damage have met limited success because of low accessibility and side effects of drugs.[12] Simple administration of the drug may not be effective in combating ROS-generated oxidative stress, as the drug gets diluted in the biological system. Therefore, it is essential to use a delivery system that can deliver increased amounts of drugs to specific organs. Liposomes and nanocapsules are well-recognized as drug vehicles, not only because of their biocompatible nature but also for their non-immunogenic property. Moreover, they cause controlled drug release and can be tailored to reach target organs.[13,14]

Melatonin (N-acetyl-5-methoxytryptamine), a natural potent antioxidant molecule, participates in maintaining circadian rhythms in animals. It may act as: 1) direct free radical scavenger,[15] 2) a stimulator of endogenous antioxidant enzymes,[16] 3) a reducer of electron discharge from the electron transport chain by lowering ROS production,[17] and 4) an augmenter of the efficiency of other antioxidants[18] against cellular oxidative injury induced by NaF.

Melatonin, having amphiphilic O-methyl and N-acetyl residues, has redox-sensitive characteristics owing to the occurrence of an electron-rich aromatic ring allowing the indole amine to act as an electron donor. Thus, melatonin can donate an electron to ·OH radicals produced by a toxicant. The reactive intermediate formed, melatoninyl cation radical, may scavenge the superoxide anion ($O_2{\cdot}^-$) to produce 3′-acetamido-2-formamido-5-methoxy-kynuramine, representing a reducing power suitable for donating two electrons. This attribute of melatonin makes it superior for preventing oxidative damage to other accessible antioxidants which have the property of donating a single electron to stabilize free radicals.[15]

Melatonin is a small hydrophobic compound, and can penetrate cell membranes and other biological barriers quite easily.[19–21] But melatonin is not acceptable as a drug scavenger because of its lipophilic property. Thus, vesicular forms such as liposome and nanocapsules, may be suitable for delivery of melatonin, reducing its toxicity by entrapping small amounts of the drug and targeting it maximally to specific sites of interest. Vesicles also ensure longer bioavailability by shielding the drug from metabolic degradation, and higher cellular permeability despite poor water solubility by improving circulation time and preventing the drug from getting diluted.[14,22]

Based on all these points, the objectives of our in vivo investigations were to assess the therapeutic efficacies of melatonin encapsulated liposomes and nanocapsules against NaF-induced oxidative toxicity and inflammation in rat liver and lungs.

Materials and methods

Chemicals

Phosphatidylethanolamine (PE), cholesterol, dicetyl phosphate (DCP), stearylamine, poly (D,L-lactide-co-glycolide) (PLGA) (molecular weight: 50,000–75,000; lactide:glycolide 85:15), and didodecyl dimethyl ammonium bromide (DDAB), bovine serum albumin (BSA), 2,6-dichloroindophenol (DCIP), phenazine methosulfate (PMS), and succinic acid were obtained from Sigma-Aldrich Co. (St Louis, MO, USA). Chloromethyl derivative of 2′,7′-dichlorodihydrofluorescein diacetate (CM-H_2DCFDA) was obtained from Thermo Fisher Scientific (Waltham, MA, USA). Ethyl acetate (EA; AR grade) was obtained from Rankem Fine Chemicals (New Delhi, India). Methanol and chloroform were obtained from E Merck (Darmstadt, Germany). Both melatonin and NaF were obtained from MP Bio medicals, LLC (Santa Ana, CA, USA). Other chemicals used were of analytical grade.

Preparation of liposomal melatonin

Two types of liposomes were prepared to target two different organs; DCP and stearylamine were used to target liver and lung tissue, respectively. Multi-lamellar liposomes were

made with PE, cholesterol, DCP/stearylamine, and melatonin in the molar ratio of 7:1:1:1.[13] Briefly, PE, cholesterol, DCP/stearylamine, and melatonin were dissolved in a mixture of methanol and chloroform (1:2 v/v) in a round-bottomed flask. A thin dry coating was formed in the inner side of the flask on evaporating the organic solvents, and the flask was desiccated overnight. The dried layer was swollen in phosphate-buffered saline (PBS; pH 7.2) for 1 hour and then sonicated for 30 seconds with a probe type sonicator. The suspension was spun at 105,000× *g* in a Sorvall RC 5B Plus ultracentrifuge (Sorvall T-865 rotor; Thermo Fisher Scientific) for 1 hour, the pellet was washed twice with PBS and resuspended in 2 mL PBS.

Preparation of nanoencapsulated melatonin

To prepare melatonin encapsulated nanocapsules, a modified emulsion-diffusion-evaporation method[14] was used. In brief, melatonin (15.499 µmol/L) was dissolved in 0.5 mL EA and 36 mg PLGA was dissolved in 2 mL EA at room temperature. Both the organic solutions of PLGA and melatonin were mixed and emulsified by drop-wise addition to a 5 mL aqueous phase containing DDAB. The resultant emulsion was stirred for 3 hours at room temperature before homogenization at 15,000 rpm for 5 minutes, and again stirred in a water bath at 40°C for 2 hours. The suspension was spun at 105,000× *g* in a Sorvall RC 5B Plus ultracentrifuge utilizing a Sorvall T-865 rotor for 1 hour. The nanoencapsulated deposit was cleaned twice with Milli-Q water, re-suspended/lyophilized with previously added 20% sucrose as cryoprotectant,[23] and stored at −20°C for further use.

Determination of encapsulation efficiency and drug loading

The encapsulation efficiency of liposomal and nanoencapsulated formulations was assayed spectrophotometrically (Rayleigh UV-2601 spectrophotometer; Beijing Beifen-Ruili Analytical Instrument Co., Ltd., Beijing, People's Republic of China). The supernatants of liposomal and nanoencapsulated suspensions collected by ultracentrifugation were lyophilized and then dissolved in 2 mL methanol for 24 hours at 4°C. The encapsulation efficiency and drug loading of vesicular melatonin were measured following the formulas:

Encapsulation efficiency (%) =
[(Total amount of formulated drug − Amount of supernatant drug)/total amount of formulated drug] ×100.

Drug loading (%) =
[(Total amount of formulated drug − Amount of supernatant drug)/vesicular mass] ×100.

Study design in animal model

Thirty male Swiss albino rats (100–120 g) were sorted into six groups of five animals each. The rats were placed in a room with controlled humidity and temperature, and adapted to 12-hour light-dark cycles for 1 week. One group (normal) was administered PBS (intravenous), and the other five (experimental) groups were treated once with NaF (48 mg/kg body weight) by oral gavage. The second group was treated once with NaF alone. The third group was treated with free drug by tail vein injection (4.46 mg/kg body weight) 2 hours after exposure to NaF. The other two groups were treated with liver- and lung-targeted DCP and stearylamine liposomal melatonin (4.46 mg/kg body weight) (intravenous) 2 hours after NaF was administered. The sixth group was treated with nanoencapsulated melatonin (4.46 mg/kg body weight) (intravenous) 2 hours after administration of NaF. Each group of animals was anesthetized using urethane (1.5 g/kg, intra-peritoneal) and sacrificed 24 hours after melatonin administration. The liver and lungs were dissected and stored at −20°C. All animal work was carried out as per the guidelines and approval of the Institutional Animal Ethics Committee (Indian Institute of Chemical Biology), India, Registration Number 147/99/CPC SEA, and the guidelines of "Principles of Laboratory Animal Care" (National Institutes of Health publication number 85-23, 1985).

Preparation of ^{125}Iodinated melatonin

Melatonin was radio-iodinated using the chloramines-T method.[24] Radioactive counting was done with a γ-ray spectrometer after separating the melatonin from the reaction mixtures.[14]

Stability of ^{125}Iodinated melatonin, liposomes, and nanocapsules in vivo

Multilamellar liposomes and nanocapsules were prepared with ^{125}Iodinated melatonin ([^{125}I]-Iodomelatonin), DCP, and stearylamine as described previously. Twelve male Swiss albino rats (100–120 g), sorted into four groups of three animals each, were injected intravenously with [^{125}I]-Iodomelatonin, liposomal [^{125}I]-Iodomelatonin, or nanoencapsulated [^{125}I]-Iodomelatonin (1×10^6 cpm in 500 µL) 2 hours after NaF oral gavage. Blood was drawn through tail vein at 1.5 minutes, 4.5 minutes, 9 minutes, 17 minutes, and 30 minutes post-injection. The total radioactivity in blood

was calculated considering the total volume of blood as 6% of the total body weight. The % radioactivity in blood was plotted against time, and half-life ($t_{1/2}$) of each type of [^{125}I]-Iodomelatonin, liposomal [^{125}I]-Iodomelatonin or nanoencapsulated [^{125}I]-Iodomelatonin was calculated by the equation $t_{1/2}$ =0.693/kel (where kel is the elimination rate constant k represented as volume of distribution/clearance).[25]

Distribution of free ^{125}Iodinated melatonin and its vesicular forms in different tissues

After 30 minutes of [^{125}I]-Iodomelatonin, liposomal, or nanoencapsulated [^{125}I]-Iodomelatonin administration, the rats were sacrificed through cervical dislocation and the amount of radioactivity in each tissue was determined with a γ-ray spectrometer and expressed as % uptake of total amount of injected dose per g of tissue.

Estimation of in vitro stability of liposomes using 6-carboxyfluorescein (6-CF)

Liposomal stability was assessed using 6-CF-encapsulated liposomes. Liposomal encapsulated 6-CF suspension (300 µL) was added to 1,200 µL PBS (pH 7.2) and rat plasma respectively, and incubated for 0–3 hours. Fluorescence was measured, after lysing the 6-CF-entrapped liposomes with 10% Triton-X-100, with a fluorescence spectrometer (Perkin Elmer LS-3; PerkinElmer Inc., Waltham, MA, USA) at excitation wavelength of 490 nm and emission wavelength of 520 nm. For each time point, the initial fluorescence (F_0) and final fluorescence (F_T) were recorded and % latency was calculated using the formula:[26]

$$\text{Latency (\%)} = [(F_T - F_0)/F_T] \times 100$$

Liposome and nanocapsule characterization using atomic force microscopy (AFM)

AFM was accomplished with an Agilent Technologies, 5500 Pico Plus AFM system (Agilent Technologies, Santa Clara, CA, USA). All the images were taken with the acoustic mode using cantilevers possessing resonance frequency 146–236 kHz, tip height 10–15 µm, and tip length 225 µm. Sample suspensions deposited on freshly cleaved mica were dried in air (65% humidity) for 30 minutes. Images were captured and analyzed with Picoview 1.10.4 version software (Molecular Imaging Corporation, San Diego, CA, USA).

Liposome characterization using scanning electron microscopy (SEM)

A JSM-6360 (JEOL, Tokyo, Japan) was used for SEM. The liposomal samples were put on specimen stubs coated with carbon tape, dried and made a thin film of palladium by a fully automated vacuum and sputter coater (JEOL Smart Coater). The sample was loaded in the air-locked specimen chamber drawer; the vacuum was maintained at 10-5 Torr range. The high energy beam was focused on the sample and image was captured.

Isolation of mitochondria

Lung and liver mitochondria were separated using differential centrifugation.[27] Liver and lungs were quickly removed from euthanized rats and homogenized in 0.23 M mannitol, 15 mM 3-(N-morpholino)propanesulfonic acid potassium hydroxide (pH 7.2), and 0.07 M sucrose buffer at a ratio of 9 mL buffer/1 g of tissue by a homogenizer with a Teflon pestle. The homogenate was spun at 700× *g* for 10 minutes and the supernatant at 8,000× *g* for 10 minutes to yield the mitochondrial pellet. The mitochondrial fraction was washed with the same buffer and frozen in liquid N_2. To obtain sub-mitochondrial membranes which are required for the determination of enzyme activities and protein estimation, the mitochondria were frozen and thawed twice, and homogenized by passage through a 15/10 tuberculin needle.[14]

Succinate dehydrogenase (SDH) activity

The activity of SDH enzyme was determined at 30°C by the PMS-mediated reduction of DCIP following the method described by Elingold et al.[28] Specific activity was expressed as units per mg of protein.

Nicotinamide adenine dinucleotide oxidase activity assay

Nicotinamide adenine dinucleotide hydride (NADH) oxidase activity of sub-mitochondrial particles (0.2 mg/mL) was determined by measuring the oxidation of NADH at 340 nm at 30°C.[28]

Membrane fluidity

Fluorescence depolarization of diphenyl hexatriene was measured to observe fluidity changes of the sub-mitochondrial membrane accompanying the gel-to-liquid crystalline phase transition.[14]

Membrane potential

Cell membrane potential was estimated by rhodamine 123 fluorescence[28] at 498 nm excitation and 525 nm emission in a Perkin Elmer LS-3B spectrofluorometer (PerkinElmer Inc.).

Measurement of ROS

Intracellular ROS in liver and lung tissue was measured[14] using a probe, CM-H_2DCFDA. Fluorescence was estimated at 499 nm excitation and 520 nm emission wavelengths in a spectrofluorometer (LS-3B, PerkinElmer Inc.)

Measurement of lipohydroperoxide level

Lung or liver tissue was homogenized in ethylenediaminetetraacetate-PBS (10% w/v). The amount of conjugated dienes formed by lipid peroxidation was expressed as μmol lipohydroperoxide/mg protein following the earlier method.[14]

Assay of cytosolic enzymes and reduced glutathione (GSH)

Lung or liver homogenates were centrifuged at 10,000× *g* for 15 minutes, followed by centrifugation of the supernatant at 105,000× *g* for 1 hour, to obtain the cytosol fraction. The catalase activity was determined spectrophotometrically at 660 nm followed by calculating the rate of degradation of H_2O_2.[14] Superoxide dismutase (SOD) activity,[29] glutathione-S-transferase (GST) activity,[27] and GSH[30] in liver and lung tissues were estimated as described previously.

Western blot

Lung or liver tissue was homogenized (10% w/v) in a lysis buffer (100 mM tris [pH 7.4], 150 mM sodium chloride, 1% triton X-100, 1% sodium deoxycholate, 0.1% sodium dodecyl sulfate, 5 mM ethylenediaminetetraacetate, 1 mM phenylmethylsulfonyl fluoride, 5 μg/mL protease inhibitor cocktail) using a Dounce homogenizer at 4°C. The homogenates were spun at 15,000× *g* for 15 minutes. The supernatant cytosolic fractions were mixed with Laemmli dye, boiled for 5 minutes, and run on sodium dodecyl sulphate-12.5% polyacrylamide gels at 100 V, followed by electrophoretic transfer to polyvinylidene fluoride membrane (EMD Millipore, Billerica, MA, USA) at 15 V for 20 minutes in a Trans-Blot semi-dry blotting apparatus (Bio-Rad Laboratories Inc., Hercules, CA, USA). The membrane was blocked with BSA in PBS and incubated with the primary anti-TNF-α or TGF-β antibody (1:500 dilution) and secondary alkaline phosphatase-conjugated rabbit anti-goat IgG antibody (1:10,000 dilution). Protein bands were visualized by using 5-bromo-4-chloro-3-indolyl-phosphate/nitroblue tetrazolium substrate solution (Sigma-Aldrich Co.) and the intensities were expressed as relative pixel densities using the Image J software system (National Institutes of Health, Bethesda, MD, USA).

Statistical analysis

Statistical analysis was carried out with one-way analysis of variance with post hoc Tukey's test using SPSS software Version 15.0 (SPSS Inc., Chicago, IL, USA). In all cases minimum significant level was kept at $P<0.05$.

Results

Bioavailability of stearylamine/DCP-liposomal and nanoencapsulated [^{125}I]-Iodomelatonin in blood plasma

The bioavailability of liposomal and nanoencapsulated [^{125}I]-Iodomelatonin is shown in Figure 1A. It was observed that stearylamine- and DCP-liposomal [^{125}I]-Iodomelatonin had circulation times of ~5.6 minutes and ~5.3 minutes respectively, whereas for nanoencapsulated [^{125}I]-Iodomelatonin the circulation time was ~11.9 minutes, compared to ~4.6 minutes for free [^{125}I]-Iodomelatonin. The values of % radioactivity varied significantly for the liposomal and nanoencapsulated forms compared to those for [^{125}I]-Iodomelatonin ($P<0.05$, $P<0.01$, and $P<0.001$).

Distribution of [^{125}I]-Iodomelatonin and its liposomal/nanoencapsulated forms in different tissues

The distribution of free, liposomal, and nanoencapsulated [^{125}I]-Iodomelatonin in tissues is shown in Table 1 and Figure 1B. The uptake of DCP-liposomal and nanoencapsulated [^{125}I]-Iodomelatonin was more ($P<0.001$) compared to [^{125}I]-Iodomelatonin, whereas the uptake of stearylamine-liposomal [^{125}I]-Iodomelatonin was less ($P<0.01$) in the liver. In the spleen, the same significant pattern was observed as described for the liver. The uptake of DCP, stearylamine-liposomal, and nanoencapsulated [^{125}I]-Iodomelatonin was more ($P<0.001$) compared to [^{125}I]-Iodomelatonin in the lung. In the heart, the uptake was more significant ($P<0.01$) for DCP, stearylamine-liposomal, and nanoencapsulated [^{125}I]-Iodomelatonin compared to [^{125}I]-Iodomelatonin. In the kidney, the uptake was more ($P<0.01$) for DCP, stearylamine-liposomal, and nanoencapsulated [^{125}I]-Iodomelatonin compared to [^{125}I]-Iodomelatonin.

Estimation of in vitro and ex vivo stability of liposomes using 6-CF as shown by % latency

It was observed that both 6-CF-loaded stearylamine and DCP-liposomes were more stable in PBS (pH 7.2) than in rat plasma after 3 hours (Figure 1C). Fifty percent latency of liposomes in the plasma required ~2 hours and ~1.8 hours, respectively. The % latency for both 6-CF-loaded stearylamine and DCP-liposomes in rat plasma was significant ($P<0.001$) at 1–3 hours compared to the value for PBS, except at initial times when $P<0.01$.

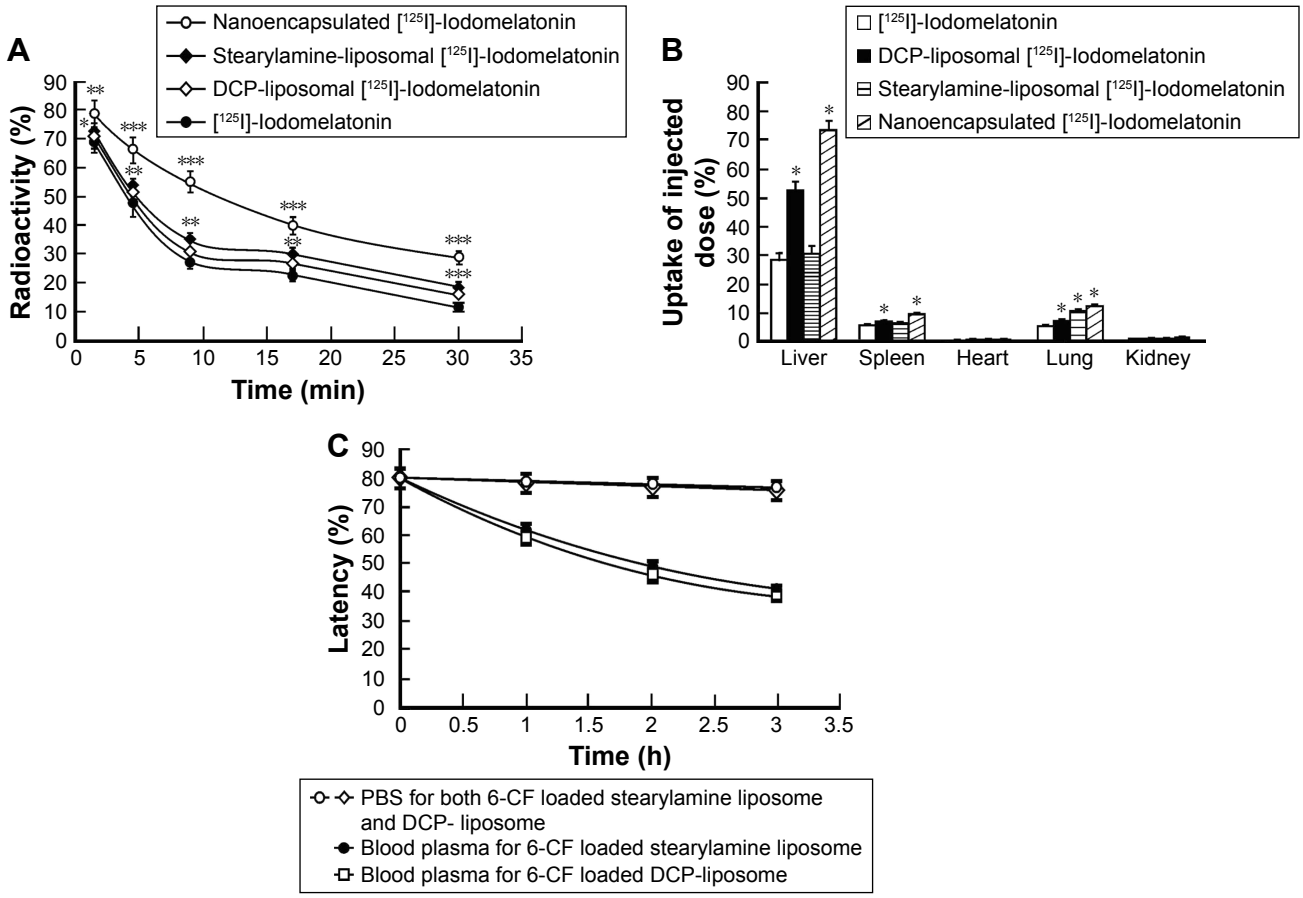

Figure 1 In vivo stability and half-life of free, charge-specific liposomal and nanoencapsulated [^{125}I]-Iodomelatonin in circulatory system (**A**), in vivo uptake of free, charge-specific liposomal and nanoencapsulated [^{125}I]-Iodomelatonin in different organs (**B**), in vitro and ex vivo release profiles of 6-CF encapsulated in charge-specific liposomes in PBS and in rat plasma (**C**). Data indicate the mean ± standard deviation of three animals. All vesicular groups were compared with [^{125}I]-Iodomelatonin, where *P<0.05, **P<0.01 and ***P<0.001 (**A**); *P<0.001, otherwise P<0.01 (**B**); for (**C**), % latency of stearylamine- and DCP-liposomal 6-CF in rat plasma was compared to PBS value at 1–3 hours where P<0.001 except at 0 hour, P<0.01.

Abbreviations: [^{125}I]-Iodomelatonin, ^{125}Iodinated melatonin; 6-CF, 6-carboxyfluorescein; PBS, phosphate-buffered saline; DCP, dicetyl phosphate.

In our earlier reports, the concentration of drug release from PLGA with DDAB was measured in PBS (pH 7.2) and rat plasma. A pharmacokinetics study showed that release of compounds (about 32% and 38%) occurred at 24 hours by diffusion through the polymer matrix, followed by a sustained release by diffusion and slow degradation of the hydrophobic polymer matrix by hydrolytic cleavages of the ester linkage.[14,31] On the other hand, the liposomal formulation exhibited a pattern of steady release (Figure 1C).[22]

Characterization of liposomal and nanoencapsulated melatonin

The size of the liposomes varied from 66 to 200 nm (Figure 2A and B). SEM images showed spherical-shaped liposomes loaded with melatonin with a diameter of ~170 nm. AFM images showed that liposomes were more or less spherical in shape (~114 nm and ~67 nm). Our previous studies using transmission electron microscopy (TEM), SEM, and AFM showed that the size of liposomes was larger (60–200 nm)

Table 1 Uptake of free, charge-specific liposomal and nanoencapsulated [^{125}I]-Iodomelatonin in different organs

Experimental groups	Uptake of injected dose (%)				
	Liver	Spleen	Heart	Lungs	Kidney
[^{125}I]-Iodomelatonin	28.4±2.3	5.6±0.2	0.61±0.02	5.34±0.2	0.71±0.02
DCP-liposomal [^{125}I]-Iodomelatonin	52.6±2.9*	7.1±0.26*	0.82±0.04	7.46±0.27*	0.94±0.05
Stearylamine-liposomal [^{125}I]-Iodomelatonin	30.8±2.6	6.3±0.24	0.74±0.03	10.62±0.32*	0.82±0.04
Nanoencapsulated [^{125}I]-Iodomelatonin	73.7±3.2*	9.2±0.29*	0.94±0.06	12.01±0.42*	1.4±0.08

Notes: Mean ± standard deviation (n=3) values for DCP/stearylamine-liposomal/nanoencapsulated [^{125}I]-Iodomelatonin were compared with those of free [^{125}I]-Iodomelatonin, *P<0.001, otherwise P<0.01.

Abbreviations: [^{125}I]-Iodomelatonin, ^{125}Iodinated melatonin; DCP, dicetyl phosphate.

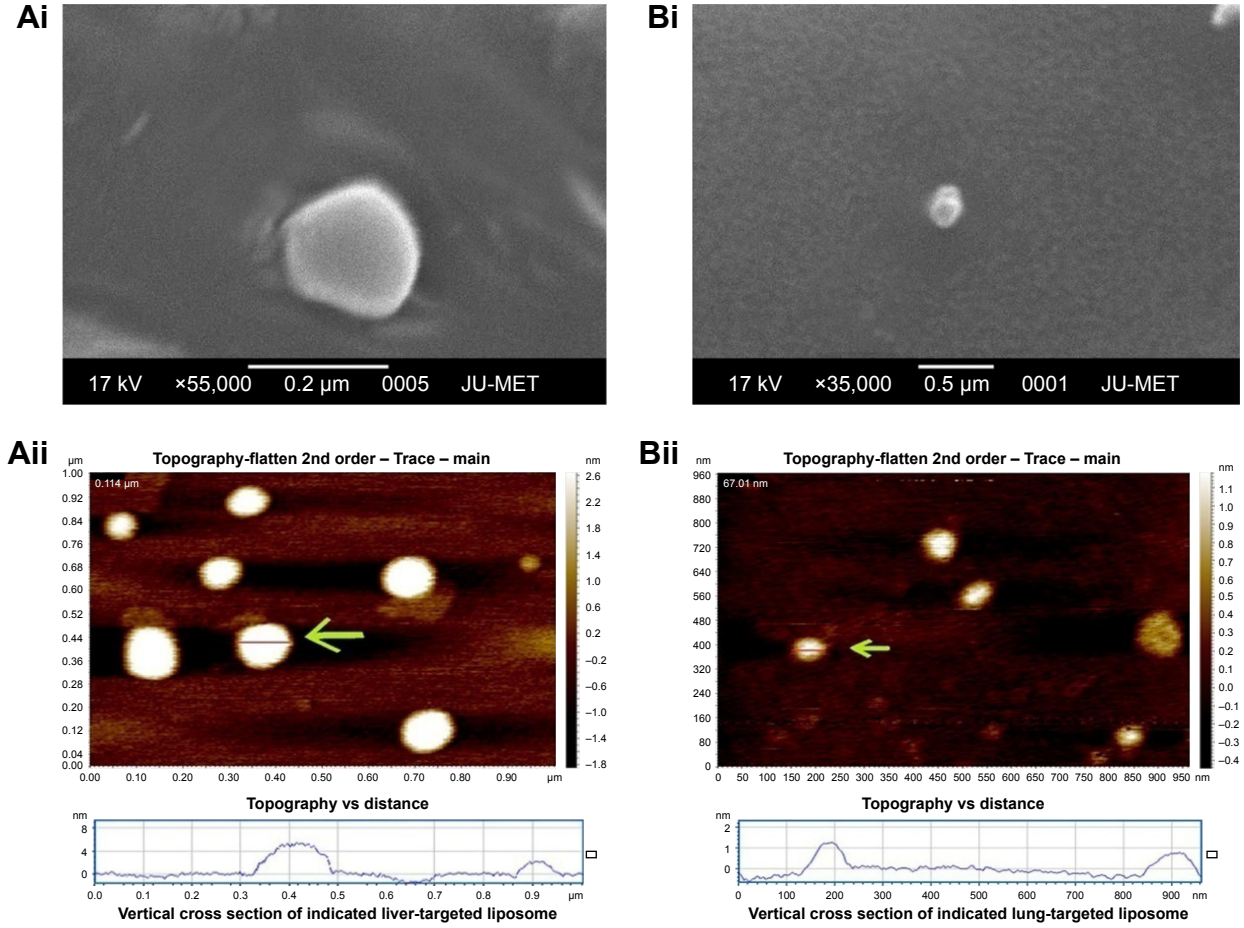

Figure 2 Characterization of liver- and lung-targeted liposomal melatonin. SEM images of melatonin-loaded DCP-liposome (**Ai**) and stearylamine liposome (**Bi**) at a magnification of 55,000× and 35,000× were captured. AFM images of melatonin-loaded DCP/stearylamine liposomes at a magnification of 1×1 µm/0.96×0.96 µm (**Aii**)/(**Bii**) were obtained 2 minutes after coating on mica sheet. Charge-specific liposomal melatonin is shown by topography-flattened views. Vertical cross sections denote the height of the specific liposomes from the mica support. The arrows in **Aii** and **Bii** indicate the diameters of DCP-liposome and stearylamine liposome, respectively.
Abbreviations: SEM, scanning electron microscopy; DCP, dicetyl phosphate; AFM, atomic force microscopy.

compared to nanocapsules (6–100 nm), both having a spherical shape.[14,22,32–35] Topological analysis by AFM demonstrated greater heights of liposomes (~4 nm) (Figure 2) compared to nanocapsules (~2 nm).[22] Even though liposomes and nanocapsules were both spherical, nanocapsules were narrower in size distribution in comparison to liposomes.

The entrapment efficiency of melatonin was higher in liposomes (~82%±4.2%) compared to nanocapsules (~69%±3.4%), while the drug loading of melatonin was higher in the liposomes (~7.45%) compared to nanocapsules (~6.86%).

ROS levels in rat liver and lungs

The fluorescence intensities generated by oxidation of CM-H_2DCFDA to DCF were proportional to the amount of ROS generated in the cells. ROS generation was increased (~2.6- and ~3.4-fold, respectively) in the liver and lungs of NaF-treated rats in comparison to normal rats. Rats treated with free melatonin after NaF exposure showed ~1.1- and ~1.5-fold decrease respectively in ROS production compared to NaF treatment. In rats treated with melatonin-loaded DCP/stearylamine liposomes, ROS productions exhibited higher diminished values (~1.6- and ~2.8-fold, respectively) compared to NaF-induction, where the nanoencapsulated melatonin treatment showed maximum decrements (~2.4- and ~3.4-fold, respectively) in rat liver and lungs (Figure 3A).

Effects of melatonin-loaded liposomes/nanocapsules on NaF-induced lipid peroxidation in liver and lungs

To investigate the degree of damage in NaF-treated rats, the values of lipohydroperoxides were monitored in rat liver and lung homogenates. The effects of free melatonin and DCP/stearylamine-liposomal and nanoencapsulated melatonin on increments in the amount of lipohydroperoxides in NaF-administered rats are demonstrated in Figure 3B. Data indicate that lipohydroperoxide levels were enhanced

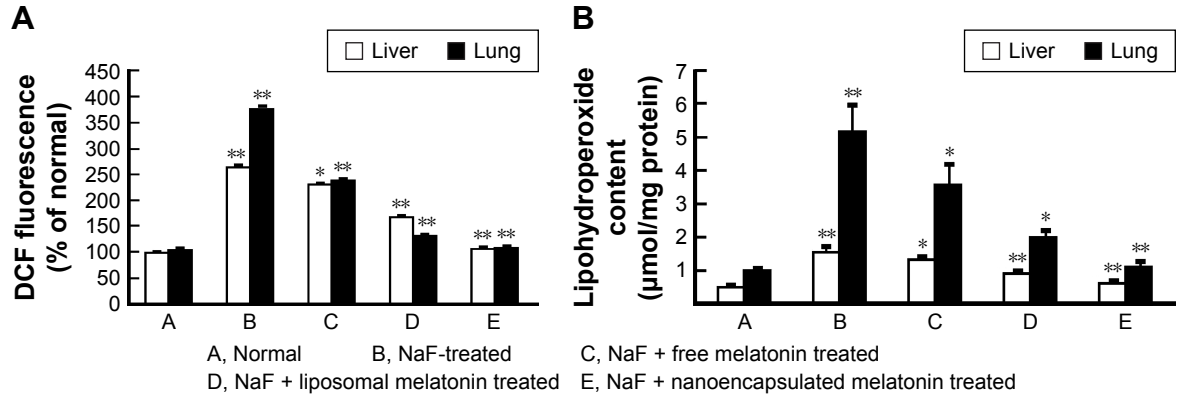

Figure 3 Evaluation of ROS (DCF fluorescence) (**A**) and conjugated dienes (lipohydroperoxides) (**B**) in rat liver and lungs. NaF-treated rats were compared with normal rats, whereas melatonin-administered rats were compared with the NaF-treated rats. Data represent mean ± standard deviation of five animals; *$P<0.01$, **$P<0.001$.
Abbreviations: DCF, 2′,7′-dichlorofluorescein; NaF, sodium fluoride; ROS, reactive oxygen species.

(~2.8/~5.1-fold) by the administration of NaF orally in contrast to normal values. Free melatonin resulted in less inhibition (~1.2/~1.4-fold) against NaF-induced liver and lung toxicities compared to NaF-treated animals. Lipohydroperoxide productions in the liver and lungs were markedly reduced (~1.6/~2.6-fold) by melatonin-loaded DCP/stearylamine-liposomal treatments, where the reductions (~2.4/~4.6-fold) were maximal in nanoencapsulated melatonin treatments in comparison to NaF-treated animals.

Mitochondrial respiratory complex enzyme activities

The mitochondrial NADH oxidase and SDH activities of the electron transport chain were studied in rat liver and lung cells (Figure 4A and B). NADH oxidase was increased (~2/~2.2-fold) in NaF-treated rats but the level of SDH activity was reduced (~1.7/~2.1-fold) in comparison to the normal values. Melatonin-loaded DCP/stearylamine-liposomal and nanoencapsulated treatments were able to bring the levels close (~1.3/~1.5- and ~1.4/0.6-fold decrease/increase, respectively) and closer (~1.9/~2- and ~1.5/~1.9-fold decrease/increase, respectively) to the normal values compared to the NaF-treated group. However, free melatonin treatment after oral gavage of NaF was unable to bring the levels close (~1.1/1.1- and ~1/~1.1-fold decrease/increase, respectively) to the normal values.

Changes in NaF-induced liver and lung cell membrane microviscosity

Exposure of rats to NaF caused a decrease (~1.8- and ~2-fold) in microviscosity of liver and lung cell membrane compared to the membrane from normal animals (Figure 5A). Free melatonin treatment reduced the alteration (~1- and ~1.1-fold) in liver and lung membrane microviscosity, whereas melatonin-encapsulated DCP/stearylamine-liposomal and

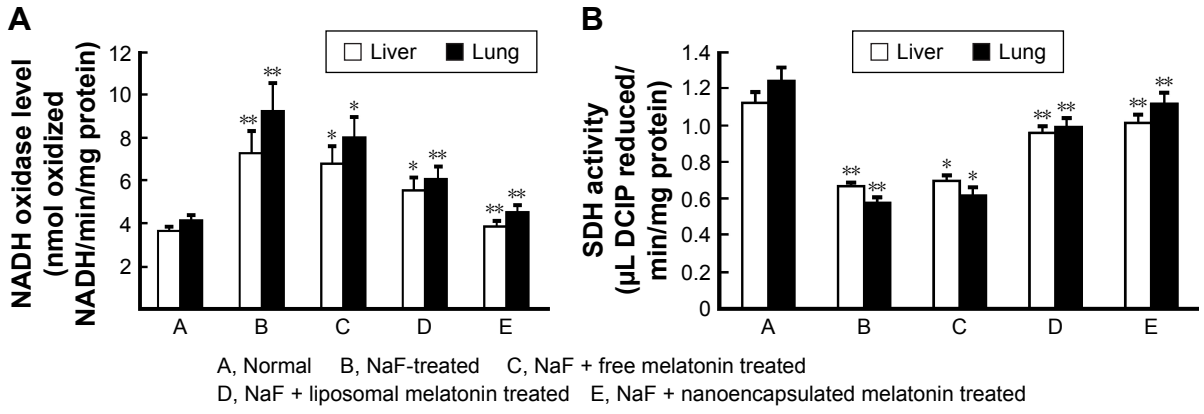

Figure 4 Effects of acute NaF-intoxication in NADH (**A**) and SDH (**B**) activities in rat liver and lungs and its regulation by liposomal/nanoencapsulated melatonin. Data show mean ± standard deviation of five rats. NaF-treated batch was compared with normal, whereas melatonin-administered batches were compared with NaF-treated batch; *$P<0.01$, **$P<0.001$.
Abbreviations: NaF, sodium fluoride; NADH, nicotinamide adenine dinucleotide hydride; SDH, succinate dehydrogenase; DCIP, 2,6-dichloroindophenol.

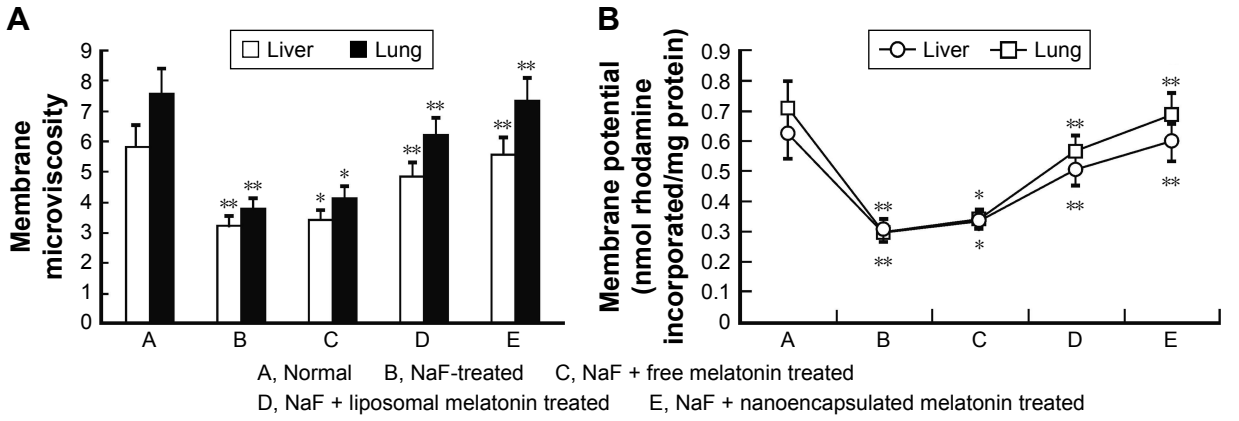

Figure 5 Evaluation of mitochondrial membrane microviscosity (**A**) and potential (**B**) in experimental rat liver and lungs. NaF-treated rats were compared with normal rats, whereas melatonin-administered rats were compared with the NaF-treated rats. Results denote mean ± standard deviation of five rats; *$P<0.01$, **$P<0.001$.
Abbreviation: NaF, sodium fluoride.

nanoencapsulated treatments inhibited liver and lung cell membrane microviscosity more (~1.5/~1.6-fold) and maximally (~1.7/~1.9-fold) compared to NaF-treated rats.

Dissipation of liver and lung cell membrane potential

NaF administration decreased (~2- and ~2.4-fold) the liver and lung cell membrane potential compared to normal values (Figure 5B). However, free melatonin treatment after NaF exposure showed less decrement (~1.1- and ~1.1-fold) in liver and lung cell membrane potential compared to NaF treatment. Appreciable and maximum repressions (~1.6/~1.9- and ~1.9/~2.3-fold, respectively) in membrane dissipation were found after melatonin-loaded DCP/stearylamine-liposomal and nanoencapsulated treatments in liver and lung cells in comparison to NaF-treated rats.

Expressions of TNF-α and TGF-β in liver and lung

The expressions of TNF-α and TGF-β after rats were gavaged orally with NaF were enhanced (~1.7/~7- and ~4.5/~1.8-fold) in liver and lung cytosol compared to normal rats, as observed by Western blot. Liposomal and nanoencapsulated melatonin treatments after NaF exposure lowered the values of TNF-α and TGF-β (~1.4/~1.6- and ~1.4/~1.2-fold and ~1.7/~3.2- and ~2.2/~2.1-fold, respectively) (Table 2; Figure 6).

Effect of liposomal/nanoencapsulated melatonin on NaF-induced changes in antioxidant defense system

The marked depletion of antioxidant activities of the endogenous antioxidant defense system, for example, GSH, GST, SOD, and catalase were assayed in NaF-treated rat lungs and liver, compared to normal counterparts (Table 3). Free melatonin treatment showed less decrement of the antioxidant activities where liposomal/nanoencapsulated melatonin treatment, after administration of NaF, exerted more/maximum enhancement of antioxidant levels in both rat liver and lungs compared to NaF-treated rats.

Effect of vesicular melatonin on NaF-induced hepatic and nephrite toxicity

The activities of hepatic and nephrite enzymes such as alkaline phosphatase, serum aspartate transaminase, urea,

Table 2 Quantifications of TNF-α and TGF-β

Experimental groups	TNF-α (pixel density)		TGF-β (pixel density)	
	Liver	Lung	Liver	Lung
Normal	18.717±0.052	5.616±0.059	11.711±0.052	29.784±0.134
NaF-treated	32.444±0.979	39.223±1.212	52.405±1.242	54.08±1.452
NaF + liposomal melatonin treated	22.327±0.337	24.629±0.601	36.286±0.602	44.013±0.886
NaF + nanoencapsulated melatonin treated	19.201±0.151	12.122±0.123	23.912±0.198	25.974±0.202

Notes: Values represent pixel densities of bands on immunoblots of liver or lung protein from animals in various experimental groups. Data have been represented as mean ± standard deviation of five rats. NaF-treated group was compared with normal animals, and melatonin-administered animals were compared with the NaF-treated animals, $P<0.001$.
Abbreviation: NaF, sodium fluoride.

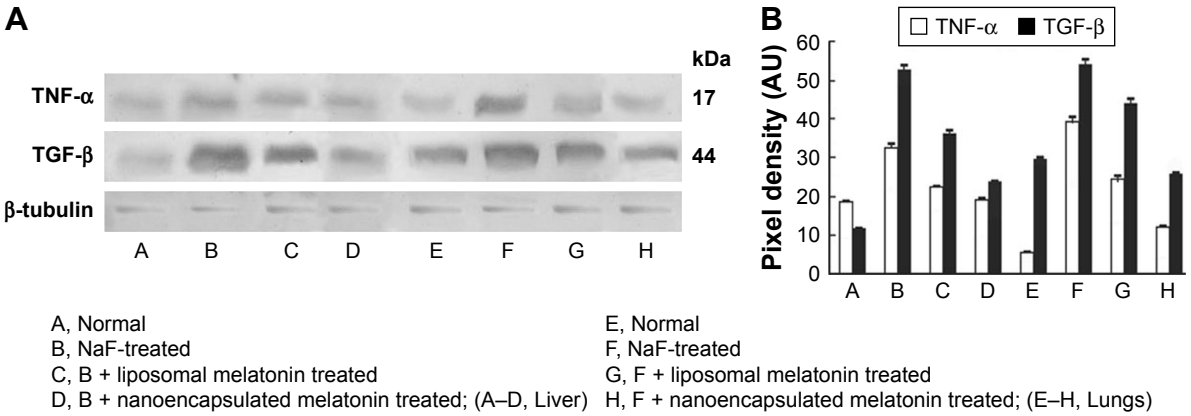

Figure 6 Western blot analysis (**A**) of TNF-α and TGF-β, demonstrated as histogram (**B**), indicating representative pixel intensities of bands on immunoblots of rat liver and lung protein. Data represent mean ± standard deviation of five rats. NaF-treated rats were compared with normal rats and the melatonin-administered rats were compared with the NaF-treated rats, where $P<0.001$.
Abbreviation: NaF, sodium fluoride.

and creatinine in serum were determined in all groups of rats (Table 4). Rats exposed to NaF showed a remarkable increase in all the activities in comparison to normal rats. The activities were reduced more/maximally by the treatment of DCP/stearylamine-liposomal and nanoencapsulated melatonin respectively.

Discussion

Liposomes and nanocapsules were found to be more stable in PBS than in plasma, as demonstrated by a lower percentage of liberation of the entrapped component into the medium, due to interactions with the complement system[36] causing a faster disruption of the vesicles (Figure 1C).[14] Our results show that [^{125}I]-Iodomelatonin has a lower $t_{1/2}$ compared to that of its vesicular forms, indicating the faster uptake of liposomes/nanocapsules into reticuloendothelial cells,[37] and delayed clearance from circulation due to their smaller size (Figure 1A). The higher increment in uptakes of liver- and lung-specific liposome/nanocapsule-encapsulated [^{125}I]-Iodomelatonin compared to [^{125}I]-Iodomelatonin may be considered to be due to passive targeting to the NaF-injured organs (Table 1, Figure 1B).

In the course of metabolism of xenobiotic compounds causing diseases, ROS is frequently produced in different organs.[38] The present study reveals that acute intoxication with NaF causes hepatic and bronchial toxicities in rats, with various levels of severity, through the increased ROS generation (Figure 3A), indicating fluoride initiated oxidative injury. This physiopathological condition appears when production of ROS in cells by the toxic entities exceeds antioxidant defense capacity of the body, causing damage to molecules, such as lipids and proteins.[39] Antioxidant enzymes are responsible for the first line of cellular defense, as they prevent macromolecules from the oxidative damage.[40] In this study, the reduced levels and activities of GSH, SOD, catalase, and GST in lung and liver tissues were observed, probably due to interaction of fluoride with metal ions in these enzymes.[41] As a result of the impaired activity of the antioxidant protection system, H_2O_2 and lipohydroperoxides accumulated in tissues, leading to injury of cellular membranes, which was reverted significantly by vesicular melatonin treatment (Table 3; Figure 3). The second line of cellular defense includes GSH to maintain the redox balance. Enhanced GSH content induced by liposomal/nanoencapsulated melatonin shows its role in reducing oxidative injuries in rat lungs and liver caused by an acute dose of fluoride (Table 3).

Exposure to fluoride hampers the normal activity of an electron transporter, ubiquinone, in the respiratory chain, inducing ROS generation.[42] Respiratory mitochondrial complex I has NADH oxidase activity, whereas complex II has SDH activity. The increased activation of NADH oxidase by the exposure of NaF (Figure 4A) indicates higher ROS generation correlating with a damaged mitochondrial electron transport system, contributing to mitochondria-related diseases.[43] Reduced activity of SDH after treatment with NaF (Figure 4B) indicates reduced electron transport through $FADH_2$ (1,5-dihydro flavin adenine dinucleotide), resulting in dissipation of membrane potential (Figure 5B). The drop in membrane potential was also accompanied by a decrease in membrane microviscosity (Figure 5A) in liver and lungs, probably owing to the accumulation of oxidatively damaged lipids and proteins, which was reverted significantly by treatment with charge-specific liposomal or nanoencapsulated melatonin.

Table 3 Impact of vesicular melatonin on antioxidative defense system in NaF-induced damage in rat liver and lungs

Experimental groups	Reduced GSH (µg GSH/mg tissue)		GST (U/mg protein)		SOD (percentile autoxidation of pyrogallol)		Catalase (µmol H_2O_2 reduced/min/mg protein)	
	Liver	Lungs	Liver	Lungs	Liver	Lungs	Liver	Lungs
Normal	12.031±1.215	14.691±1.276	1.142±0.071	1.261±0.082	47.291±3.792	49.383±4.278	6.307±0.593	8.047±0.785
NaF-treated (A)	6.587±0.413	8.586±0.572	0.617±0.022	0.745±0.031	24.814±1.215	26.692±1.362	3.726±0.164	4.207±0.201
A + free melatonin treated	7.642±0.605	9.683±0.669	0.715±0.035	0.821±0.044	26.427±1.475	28.376±1.621	4.271±0.196	5.316±0.235
A + liposomal melatonin treated	9.754±0.837	12.795±0.915	0.891±0.051	1.041±0.063	37.568±2.031	39.145±2.482	5.628±0.386	7.231±0.437
A + nanoencapsulated melatonin treated	11.576±0.978	13.763±7.062	0.989±0.062	1.112±0.073	44.342±3.416	45.864±3.987	6.012±0.525	7.893±0.667

Notes: Data have been shown as mean ± standard deviation of five rats. NaF-treated batch was compared to normal animals, whereas melatonin-administered batches were compared with the NaF-treated batch; $P<0.001$.
Abbreviations: NaF, sodium fluoride; GSH, glutathione; GST, glutathione-S-transferase; SOD, superoxide dismutase.

Fluoride-induced inflammation inhibited by vesicular melatonin, was observed in our study (Table 2; Figure 6). Kupffer/macrophage cells may intervene in the second phase of hepatic and bronco-cellular damage induced by ROS intermediates,[44] and activate prime Ito cells for production of augmented extracellular matrix components during fibrogenesis mediated by TGF-β (Table 2; Figure 6).[45] Thus, cytokines and few other factors, for example, TNF-α (Table 2; Figure 6)[46,47] may take part in the injury of reticuloendothelial cells.

For hepatic/bronchial cellular injury, melatonin-loaded vesicles, competent to target their cargo to the effected cells, may be used for maximum therapeutic efficacy in comparison to free melatonin treatment (Tables 1–4; Figures 1–6).[48] To increase site specificity to the liver, DCP was used because it possesses −ve charge attracted to +vely charged liver cells, while cationic liposomes containing stearylamine were used to target −vely charged bronchial cells via endocytosis.[49–51] Nanoencapsulation of melatonin in PLGA stabilized with cationic surfactant DDAB, was found to be the most effective in preventing NaF-induced oxidative injury in rat liver and lungs, as these nanoparticles are transported to −vely charged lysosomes, followed by their rapid accumulation in the electron-dense mitochondria.[52–56]

Melatonin, an indole amine neurohormone, may exert a regulatory function as a lipophilic antioxidant (Table 1; Figures 3A and 4A), with anti-inflammatory activities (Table 2; Figure 6).[57] The interactions of melatonin with ROS (mainly ·OH), indicate the potent free radical scavenging activity, as demonstrated by others.[58] It may also stimulate intracellular free radical scavenger and antioxidant GSH to increase GSH concentration (Table 3).[57] Moreover, mitochondrial binding sites for the indole ring of melatonin may be responsible for inhibiting NADH-oxidase-dependent ROS generation, as well as lipid peroxidation induced by NaF (Figures 3A and 4A).[57]

Conclusion

Our work has revealed that NaF intoxication caused oxidative injuries, upregulation of TNF-α and TGF-β in rat liver and lungs, which may be prevented by treatment with melatonin, and especially with its vesicular forms with higher biological efficiencies. Even though clinical application of melatonin is restricted due to its lipophilicity with little bioavailability and toxicity, nanoencapsulated melatonin may be judged as an alternative remedial approach for NaF-induced poisoning because of its long shelf life, smaller size, better cellular uptake, and prolonged drug-liberating capability in vivo.[14,59,60]

Table 4 Effect of vesicular melatonin on serum markers for NaF-induced oxidative damage

Experimental groups	AP (U/L)	SAT (IU/L)	Urea (g/L)	Creatinine (mg/L)
Normal	271.467±15.14	33.978±3.82	0.43±0.04	11.6±3.01
NaF-treated (A)	620.548±31.42**	66.793±7.24**	0.86±0.08**	60.67±6.03**
A + free melatonin treated	590.163±28.64**	59.685±6.78**	0.82±0.07*	47.18±5.14**
A + DCP-liposomal melatonin treated	420.578±22.74**	44.764±5.12**	0.58±0.06**	29.19±4.52**
A + stearylamine-liposomal melatonin treated	443.692±24.23**	47.389±5.33**	0.60±0.06**	31.22±4.64**
A + nanoencapsulated melatonin treated	309.645±18.47**	36.487±4.46**	0.46±0.05**	15.46±3.82**

Notes: Data show mean ± standard deviation of five rats. The NaF-treated batch was compared with normal animals, and the melatonin-administered batches were compared with the NaF-treated batch. *$P<0.01$, **$P<0.001$.
Abbreviations: NaF, sodium fluoride; AP, alkaline phosphatase; SAT, serum aspartate transaminase; DCP, dicetyl phosphate.

Acknowledgments

This study was supported by the Council of Scientific and Industrial Research (CSIR), Government of India. The authors are thankful to Mr Muruganandan, Technical Officer, IICB, Kolkata, for atomic force microscopy. The authors are also grateful for critical language editing by Dr Samit Adhya, Emeritus Scientist, CSIR-IICB, Kolkata.

Disclosure

The authors report no conflicts of interest in this work.

References

1. Coplan MJ, Patch SC, Masters RD, Bachman MS. Confirmation of and explanations for elevated blood lead and other disorders in children exposed to water disinfection and fluoridation chemicals. *Neurotoxicology*. 2007;28(5):1032–1042.
2. Dubey N, Khan AM, Raina R. Sub-acute deltamethrin and fluoride toxicity induced hepatic oxidative stress and biochemical alterations in rats. *Bull Environ Contam Toxicol*. 2013;91(3):334–338.
3. Edmunds WM, Smedley PL. Ground water geochemistry and health: an overview. *Environmental Geochemistry and Health*. 1996;113(1): 91–105.
4. US National Research Council. *Health effects of ingested fluoride*. Washington DC: National Research Council: National Academy Press; 1993.
5. Mittal M, Flora SJ. Effects of individual and combined exposure to sodium arsenite and sodium fluoride on tissue oxidative stress, arsenic and fluoride levels in male mice. *Chem Biol Interact*. 2006;162(2):128–139.
6. Barbier O, Arreola-Mendoza L, Del Razo LM. Molecular mechanisms of fluoride toxicity. *Chem Biol Interact*. 2010;188(2):319–333.
7. Shivarajashankara YM, Shivashankara AR, Gopalakrishnan BP, Rao SH. Brain lipid peroxidation and antioxidant systems of young rats in chronic fluoride intoxication. *Fluoride*. 2002;35(3):197–203.
8. Birkner E, Grucka ME, Machoy Z, Tamawski R, Polaniak R. Disturbance of protein metabolism in rats after acute poisoning with sodium fluoride. *Fluoride*. 2000;33(4):182–186.
9. Chlubek D, Poland S. Fluoride and oxidative stress. *Fluoride*. 2003;36(4): 217–228.
10. Shivarajashankara YM, Shivashankara AR, Gopalakrishnan BP, Rao SH. Effect of fluoride intoxication on lipid peroxidation and antioxidants system in rats. *Fluoride*. 2001;34(2):108–113.
11. Shuhua X, Ziyou L, Ling Y, Fei W, Sun G. A role of fluoride on free radical generation and oxidative stress in BV-2 microglia cells. *Mediators Inflamm*. 2012;2012:102954.
12. Chinoy NJ, Memon MR. Beneficial effects of some vitamins and calcium on sodium fluoride and aluminium toxicity on gastrocnemius muscle and liver of male mice. *Fluoride*. 2001;34(1):21–23.
13. Mandal AK, Das S, Basu MK, Chakrabarti RN, Das N. Hepatoprotective activity of liposomal flavonoid against arsenite-induced liver fibrosis. *J Pharmacol Exp Ther*. 2007;320(3):994–1001.
14. Mandal AK, Ghosh D, Sarkar S, Ghosh A, Swarnakar S, Das N. Nanocapsulated quercetin downregulates rat hepatic MMP-13 and controls diethylnitrosamine-induced carcinoma. *Nanomedicine (Lond)*. 2014;9(15):2323–2337.
15. Allegra M, Reiter RJ, Tan DX, Gentile C, Tesoriere L, Livrea MA. The chemistry of melatonin's interaction with reactive species. *J Pineal Res*. 2003;34(1):1–10.
16. Rodriquez C, Mayo JC, Sainz RM, et al. Regulation of antioxidant enzymes: a significant role for melatonin. *J Pineal Res*. 2004; 36(1):1–9.
17. Acuna-Castroviejo D, Escames G, Carozo A, Leon J, Khaldy H, Reiter RJ. Melatonin, mitochondrial homeostasis and mitochondrial-related diseases. *Curr Top Med Chem*. 2002;2(2):133–152.
18. Gitto E, Tan DX, Reiter RJ, et al. Individual and synergistic actions of melatonin: studies with vitamin E, vitamin C, glutathione and desferoxamine in liver homogenates. *J Pharm Pharmacol*. 2001;53(10):1393–1401.
19. Yu H, Dickson EJ, Jung SR, Koh DS, Hille B. High membrane permeability for melatonin. *J Gen Physiol*. 2016;147(1):63–76.
20. Hardeland R. Antioxidative protection by melatonin: multiplicity of mechanisms from radical detoxification to radical avoidance. *Endocrine*. 2005;27(2):119–130.
21. Reiter RJ, Manchester LC, Tan DX. Neurotoxins: free radical mechanisms and melatonin protection. *Curr Neuropharmacol*. 2010;8(3): 194–210.
22. Choudhury ST, Das N, Ghosh S, Ghosh D, Chakraborty S, Ali N. Vesicular (liposomal and nanoparticulated) delivery of curcumin: a comparative study on carbon tetrachloride-mediated oxidative hepatocellular damage in rat model. *Int J Nanomedicine*. 2016;11:2179–2193.
23. Abdelwahed W, Degobert G, Stainmesse S, Fessi H. Freeze-drying of nanoparticles: formulation, process and storage considerations. *Adv Drug Deliv Rev*. 2006;58(15):1688–1713.
24. Opresko L, Wiley HS, Wallace RA. Protein iodinated by the chloramines-T method appear to be degraded at an abnormally rapid rate after endocytosis. *Proc Natl Acad Sci U S A*. 1980;77(3):1556–1560.
25. Soliman AM, Ayad ARA. Pharmacokinetics and efficacy of tilmicosin in the treatment of Pasteurella haemolytica bronchopneumonia in calves. *Pharmacol Pharm*. 2014;5:514–523.
26. Bors W, Hiller W, Michel C, Saran M. Flavonoids as antioxidants: determination of radical-scavenging efficiencies. *Methods Enzymol*. 1990;186:343–355.
27. Navarro A, Boveris A. Rat brain and liver mitochondria develop oxidative stress and lose enzymatic activities on aging. *Am J Physiol Regul Integr Comp Physiol*. 2004;287(5):R1244–R1249.
28. Elingold I, Isollabella MP, Casanova MB, et al. Mitochondrial toxicity and antioxidant activity of a prenylated flavonoid isolated from Delea elegans. *Chem Biol Interact*. 2008;171(3):294–305.
29. Marklund S, Marklund G. Involvement of the superoxide anion radical in the autoxidation of pyrogallol and a convenient assay for superoxide dismutase. *Eur J Biochem*. 1974;47(3):469–474.

30. Griffith OW. Determination of glutathione and glutathione disulfide using glutathione reductase and 2-vinylpyridine. *Anal Biochem*. 1980;106(1):207–212.
31. Dinarvand R, Sepehri N, Manoochehri S, Rouhani H, Atyabi F. Polylactide-co-glycolide nanoparticles for controlled delivery of anticancer agents. *Int J Nanomedicine*. 2011;6:877–895.
32. Ghosh S, Das N, Mandal AK, Dungdung SR, Sarkar S. Mannosylated liposomal cytidine 5′ diphosphocholine prevent age related global moderate cerebral ischemia reperfusion induced mitochondrial cytochrome c release in aged rat brain. *Neuroscience*. 2010;171(4):1287–1299.
33. Ghosh S, Dungdung SR, Choudhury ST, et al. Encapsulation of the flavonoid quercetin with an arsenic chelator into nanocapsules enables the simultaneous delivery of hydrophobic and hydrophilic drugs with a synergistic effect against chronic arsenic accumulation and oxidative stress. *Free Radic Biol Med*. 2011;51(10):1893–1902.
34. Ghosh A, Sarkar S, Mandal AK, Das N. Neuroprotective role of nanoencapsulated quercetin in combating ischemia-reperfusion induced neuronal damage in young and aged rats. *PLoS One*. 2013;8(4):e57735.
35. Ghosh A, Banerjee T, Bhandary S, Surolia A. Formulation of nanotized curcumin and demonstration of its antimalarial efficacy. *Int J Nanomedicine*. 2014;9:5373–5387.
36. Socha M, Bartecki P, Passirani C, et al. Stealth nanoparticles coated with heparin as peptide or protein carriers. *J Drug Target*. 2009;17(8):575–585.
37. De Jong WH, Borm PJ. Drug delivery and nanoparticles: applications and hazards. *Int J Nanomedicine*. 2008;3(2):133–149.
38. Ray PD, Huang BW, Tsuji Y. Reactive oxygen species (ROS) homeostasis and redox regulation in cellular signaling. *Cell Signal*. 2012;24(5):981–990.
39. Bartsch H, Dally H, Popanda O, Risch A, Schmezer P. Genetic risk profiles for cancer susceptibility and therapy response. *Recent Results Cancer Res*. 2007;174:19–36.
40. Lenaz G. Mitochondria and reactive oxygen species. Which role in physiology and pathology? *Adv Exp Med Biol*. 2012;942:93–136.
41. Chinoy NJ. Fluoride stress on antioxidant defense systems. *Fluoride*. 2003;36(3):138–141.
42. Gutowska I, Baranowska-Bosiacka I, Baskiewicz M, et al. Fluoride as a pro-inflammatory factor and inhibitor of ATP bioavailability in differentiated human THP1 monocytic cells. *Toxicol Lett*. 2010;196(2):74–79.
43. Sun Z, Niu R, Wang B, et al. Fluoride-induced apoptosis and gene expression profiling in mice sperm in vivo. *Arch Toxicol*. 2011;85(11):1441–1452.
44. Brenner C, Galluzzi L, Kepp O, Kroemer G. Decoding cell death signals in liver inflammation. *J Hepatol*. 2013;59(3):583–594.
45. Gressme OA, Rizk MS, Kovalenko E, Weiskirchen R, Gressner AM. Changing the pathogenetic roadmap of liver fibrosis? Where did it start; where will it go? *J Gastroenterol Hepatol*. 2008;23(7 Pt 1):1024–1035.
46. Medrano-Engay B, Irun P, Gervas-Arruga J, et al. Iron homeostasis and inflammatory biomarker analysis in patients with type I Gaucher disease. *Blood Cells Mol Dis*. 2014;53(4):171–175.
47. Montecucco F, Mach F, Lenglet S, et al. Treatment with Evasin-3 abrogates neutrophil-mediated inflammation in mouse acute pancreatitis. *Eur J Clin Invest*. 2014;44(10):940–950.
48. Mandal AK, Sinha J, Mandal S, Mukhopadhyay S, Das N. Targeting of liposomal flavonoid to liver in combating hepatocellular oxidative damage. *Drug Deliv*. 2002;9(3):181–185.
49. Yu HY, Lin CY. Uptake of charged liposomes by the rat liver. *J Formos Med Assoc*. 1997;96(6):409–413.
50. Ishiwata H, Suzuki N, Ando S, Kikuchi H, Kitagawa T. Characteristics and biodistribution of cationic liposomes and their DNA complexes. *J Control Release*. 2000;69(1):139–148.
51. Stebelska K, Wyrozumska P, Gubernator J, Sikorski AF. Highly fusogenic cationic liposomes transiently permeabilize the plasma membrane of HeLa cells. *Cell Mol Biol Lett*. 2007;12(1):39–50.
52. Mousa SA, Bharali DJ. Nanotechnology-based detection and targeted therapy in cancer: nano-bio paradigms and applications. *Cancers (Basel)*. 2011;3(3):2888–2903.
53. Asati A, Santra S, Kaittanis C, Perez JM. Surface-charge-dependent cell localization and cytotoxicity of cerium oxide nanoparticles. *ACS Nano*. 2010;4(9):5321–5331.
54. Lemmer Y, Kalombo L, Pietersen RD, et al. Mycolic acids, a promising mycobacterial ligand for targeting of nanoencapsulated drugs in tuberculosis. *J Control Release*. 2015;211:94–104.
55. Souza LG, Silva EJ, Martins AL, et al. Development of topotecan loaded lipid nanoparticles for chemical stabilization and prolonged release. *Eur J Pharm Biopharm*. 2011;79(1):189–196.
56. Murphy MP, Smith RA. Targeting antioxidants to mitochondria by conjugation to lipophilic cations. *Annu Rev Pharmacol Toxicol*. 2007;47:629–656.
57. Reiter RJ, Tan DX, Mayo JC, Sainz RM, Leon J, Czarnocki Z. Melatonin as an antioxidant: biochemical mechanisms and pathophysiological implications in humans. *Act Biochim Pol*. 2003;50(4):1129–1146.
58. Li C, Li G, Tan DX, Li F, Ma X. A novel enzyme-dependent melatonin metabolite in humans. *J Pineal Res*. 2013;54(1):100–106.
59. Rivera S, Pala D, Bedini A, Spadoni G. Therapeutic uses of melatonin and melatonin derivatives: a patent review (2012–2014). *Expert Opin Ther Pat*. 2015;25(4):425–441.
60. Cartiera MS, Johnson KM, Rajendran V, Caplan MJ, Saltzman WM. The uptake and intracellular fate of PLGA nanoparticles in epithelial cells. *Biomaterials*. 2009;30(14):2790–2798.

International Journal of Nanomedicine Dovepress

Publish your work in this journal

The International Journal of Nanomedicine is an international, peer-reviewed journal focusing on the application of nanotechnology in diagnostics, therapeutics, and drug delivery systems throughout the biomedical field. This journal is indexed on PubMed Central, MedLine, CAS, SciSearch®, Current Contents®/Clinical Medicine, Journal Citation Reports/Science Edition, EMBase, Scopus and the Elsevier Bibliographic databases. The manuscript management system is completely online and includes a very quick and fair peer-review system, which is all easy to use. Visit http://www.dovepress.com/testimonials.php to read real quotes from published authors.

Submit your manuscript here: http://www.dovepress.com/international-journal-of-nanomedicine-journal